

Intramolecular Redox-Active Ligand-to-Substrate Single-Electron Transfer: Radical Reactivity with a Palladium(II) Complex

Daniël L. J. Broere,[†] Bas de Bruin,[†] Joost N. H. Reek,[†] Martin Lutz,[‡] Sebastian Dechert,[§] and Jarl Ivar van der Vlugt^{*,†}

[†]Homogeneous, Bioinspired & Supramolecular Catalysis, van 't Hoff Institute for Molecular Sciences, University of Amsterdam, Science Park 904, 1098 XH Amsterdam, The Netherlands

[‡]Crystal and Structural Chemistry, Bijvoet Center for Biomolecular Research, Utrecht University, 3584 CH Utrecht, The Netherlands

[§]Institut für Anorganische Chemie, Georg-August-Universität Göttingen, 37077 Göttingen, Germany

Supporting Information

ABSTRACT: Coordination of the redox-active tridentate NNO ligand L^{H2} to Pd^{II} yields the paramagnetic iminobenzosemiquinonato complex **3**. Single-electron reduction of **3** yields diamagnetic amidophenolato complex **4**, capable of activating aliphatic azide **5**. Experimental and computational studies suggest a redox-noninnocent pathway wherein the redox-active ligand facilitates intramolecular ligand-to-substrate single-electron transfer to generate an open-shell singlet “nitrene-substrate radical, ligand radical”, enabling subsequent radical-type C–H amination reactivity with Pd^{II} .

Redox-active ligands are highly relevant for many metalloenzymatic transformations, supplying electrons and facilitating selective atom transfer reactivity.¹ Synthetic analogues have recently also shown remarkable potential in enabling two-electron redox processes for bond activation and formation processes, either acting as an electron reservoir or directing radical-type reactivity when combined with transition metals.² Single-electron transfer (SET) from a redox-active ligand to a substrate without metal oxidation state change is very rare.³ Transformations mediated by palladium are dominated by two-electron processes,⁴ whereas ligand-to-substrate SET might allow selective substrate activation via a controlled radical-type mechanism while benefiting from favorable Pd-substrate coordination.

In order to induce and control this ligand-to-substrate electron transfer reactivity on a suitable stable Pd platform and to avoid ligand dissociation during the redox-state shuttling events, we integrated the redox-active 2-aminophenol⁵ ($N^{H}O^H$) unit within a tridentate $NN^H O^H$ pincer⁶ scaffold. Upon double deprotonation, this ligand may coordinate to Pd^{II} as a 2-amidophenolato dianion (NNO^{AP}), iminobenzosemiquinonato radical monoanion (NNO^{ISQ}), or a neutral iminobenzoquinone (NNO^{IBQ} , Figure 1), without formal redox changes occurring at Pd.⁷ Single-electron transfer reactivity from such an NO-fragment to exogenous electron acceptors is not described to date for any of its redox states. We envisioned that the (NNO^{AP}) state might be ideally suited to establish intramolecular ligand-to-substrate electron shuttling and to perform radical-type reactions with Pd^{II} .

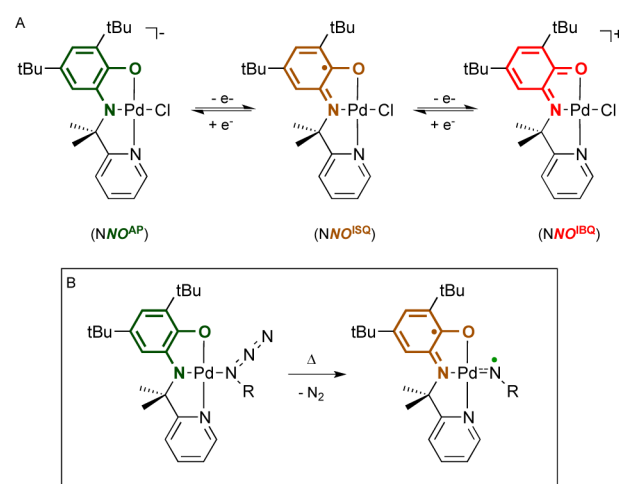


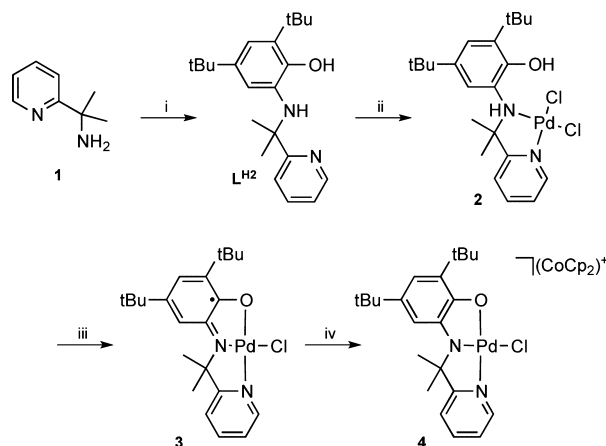
Figure 1. (A) Redox states of Pd^{II} -coordinated NNO ligand. (B) Concept of ligand-to-substrate single-electron transfer demonstrated for an azide substrate, generating a “nitrene-substrate radical, ligand radical” on Pd^{II} .

We herein report the synthesis of this new redox-active $NN^H O^H$ pincer ligand, bearing an additional pyridine donor to impart coordinative stability, the resulting air- and moisture-stable paramagnetic Pd^{II} complex ($S = 1/2$) **3**, and its one-electron reduced diamagnetic derivative **4**. The ligand-centered redox behavior of this one-electron reduced species was probed experimentally and computationally (DFT). The combined data indicate that single-electron transfer from the redox-active ligand to an organic azide occurs under thermal activation to produce a “nitrene-substrate radical, ligand-radical” Pd^{II} intermediate with an open-shell singlet (singlet diradical) ground state. As proof-of-principle reactivity with this ligand-based electron transfer concept, this unusual intermediate undergoes intramolecular sp^3 C–H amination to generate a pyrrolidine species.

The two-step synthesis of $NN^H O^H$ ligand L^{H2} involves double addition of $MeCeCl_2$ on 2-cyanopyridine⁸ to form amine **1** (Scheme 1), followed by condensation with 1,3-di(*tert*-

Received: March 3, 2014

Published: June 13, 2014

Scheme 1. Synthesis of L^{H2} , 2, 3, and 4^a

^aReagents: (i) DTBQ, DTBC, neat; (ii) $\text{PdCl}_2(\text{NCMe})_2$; (iii) NEt_3 , air; (iv) CoCp_2 .

butyl)quinone to produce an iminoquinone intermediate that is reduced *in situ* by 1,3-di(*tert*-butyl)catechol.⁹ The geminal methyl and *tert*-butyl groups are incorporated in the framework to prevent β -H elimination and to stabilize the NNO^{ISQ} oxidation state upon coordination, respectively. Colorless solid $L^{\text{H}2}$ is bench-stable for months but susceptible to oxidation in solution under air, concomitant with a color change to green and broadening of the NMR signals. For reference, we also synthesized $L^{\text{H}2}$ bearing no *gem*-dimethyl groups.¹⁰

Ligand $L^{\text{H}2}$ reacts as a neutral ligand with $\text{PdCl}_2(\text{MeCN})_2$ to give orange $\text{PdCl}_2(L^{\text{H}2})$ (2) in high yield. NMR analysis suggests pyridine and $-\text{NH}$ coordination to Pd (diastereotopic $-\text{CH}_3$ groups; δ 6.58 (NH)), with no interaction of the $-\text{OH}$ group (δ 6.53).¹⁰ Addition of NEt_3 in MeOH under aerobic conditions resulted in brown paramagnetic compound 3, characterized as $\text{PdCl}(L^{\bullet})$ ($L^{\bullet} = \text{NNO}^{\text{ISQ}}$). Magnetic susceptibility measurement of 3 at 298 K using Evans' method¹¹ gave an effective magnetic moment (μ_{eff}) of 1.78 μ_{B} , indicating an $S = 1/2$ ground state. X-band EPR spectroscopy in toluene at 298 K (Figure 2, left) revealed hyperfine couplings with ^{105}Pd , ^{15}N , and two ^1H nuclei. The simulated spectrum and calculated hyperfine couplings

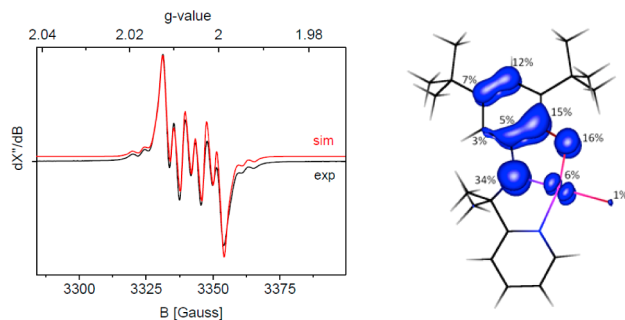


Figure 2. Left: Experimental and simulated EPR spectrum of 3. Microwave frequency = 9.382892 GHz. Power = 2 mW. Modulation amplitude = 0.1 G. Simulated (DFT) g value and hyperfine couplings A (MHz): g_{iso} 2.0055 (2.0059); $A_{\text{iso}}^{\text{Pd}}$ +12.8 (+10.7); $A_{\text{iso}}^{\text{N}}$ +22.8 (+17.1); $A_{\text{iso}}^{\text{H}1}$ -10.6 (-7.9); $A_{\text{iso}}^{\text{H}2}$ -2.8 (-2.4). DFT parameters: ORCA (b3-lyp/def2-TZVP). Right: DFT (b3-lyp/def2-TZVP) calculated spin-density plot for 3.

correlate well with the experimental data. The g_{iso} value of 2.0055 supports an NNO^{ISQ} ligand radical coordinated to Pd^{II} . The calculated spin-density plot for 3 (93% total spin density, 34% on the iminosemiquinonato nitrogen) is in agreement with EPR data (Figure 2, right).

The molecular structure of 3 (Figure 3) shows metric parameters that are characteristic for the (*N*) NO^{ISQ} ligand

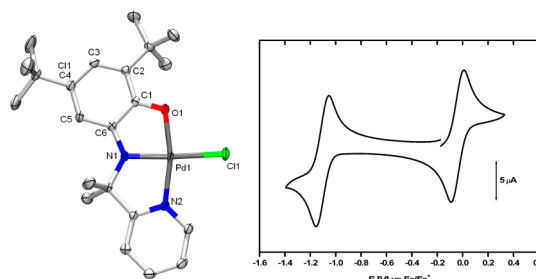


Figure 3. Top left: Displacement ellipsoid plot (50% probability level) of 3. H atoms and solvent omitted for clarity.¹¹ Top right: Cyclic voltammogram of 3 in CH_2Cl_2 (10^{-3} M); scan rate 200 mV s^{-1} ; referenced to Fc/Fc^+ . Bottom: Relevant XRD metric parameters of 3 (left) and 4 (right).

oxidation state.¹² DFT (b3-lyp/def2-TZVP) calculated optimized geometric parameters for the doublet NNO^{ISQ} ground state matched well with the experimentally found values.¹⁰ Cyclic voltammetry of 3 in CH_2Cl_2 solution revealed fully reversible one-electron oxidation and reduction events at +0.04 V and -1.11 V vs Fc/Fc^+ , respectively (Figure 3, right). Chemical reduction of 3 with CoCp_2 in CH_2Cl_2 furnished $[\text{CoCp}_2][\text{PdCl}(\text{NNO}^{\text{AP}})]$ as soluble, air-sensitive diamagnetic species 4. Single crystals were obtained by reactive diffusion of a CoCp_2 solution into a solution of 3 in benzene. The anionic portion of this complex is almost isostructural to 3 (Figure 3), showing an elongated Pd-Cl bond and characteristic bond lengths for the (*N*) NO^{AP} oxidation state that matched well with DFT calculated metric parameters. Synthesis of the neutral analogue **4PPh₃** was achieved by addition of 1 equiv of PPh_3 to either the *in situ* reduction of 3 or preformed 4.¹⁰

We anticipated that the reduced nature of the NNO^{AP} scaffold in species 4 could be utilized to generate an unpaired electron at a coordinated substrate by unprecedented intramolecular ligand-to-substrate SET on Pd^{II} . To support this hypothesis, we performed DFT calculations on 4 with model azide N_3^{Et} . MO plot analysis showed that loss of N_2 concomitant with SET from the NNO^{AP} ligand to the nitrene substrate is indeed accessible, generating a rare "nitrene-substrate radical,^{13,14} ligand-radical" Pd^{II} species 5N^{R} with an open-shell singlet (singlet diradical) ground state. 5N^{R} bears 87% α -spin density at the nitrene N-atom (Figure 4; left: HOMO for 4N_3^{R} , right: spin density distribution for 5N^{R}).

To exploit this concept of ligand-based single-electron transfer to generate a substrate radical, we investigated the reactivity of these $\text{Pd}(\text{NNO})$ complexes in radical-type sp^3 C-H amination.¹⁵ These reactions often proceed via a radical-type mechanism involving C-H abstraction followed by a radical-

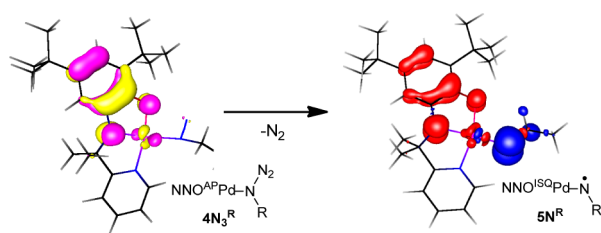
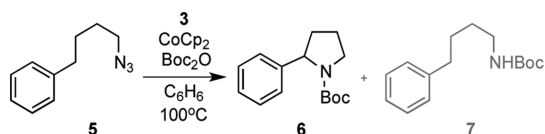


Figure 4. DFT (b3-lyp/def2-TZVP) calculated HOMO plot for model complex $4N_3^R$ (left) and spin-density plot for model diradical $5N^R$ (right) with blue: positive (α) and red: negative (β) spin density. R = ethyl.

rebound step, or alternatively via direct insertion of the radical nitrene fragment in the C–H bond. The Fe-mediated C–H amination of unactivated alkyl azides occurs via a radical pathway involving metal-based redox chemistry,¹⁶ but a ligand-induced radical pathway for this reaction has never been disclosed. Upon reduction of **3** to **4** with cobaltocene in the presence of unactivated azide **5** and Boc₂O, pyrrolidine **6** (~1 equiv with respect to **4**), and the reduced Boc-protected amine **7** were observed (Scheme 2). Use of **4PPh₃**, Pd₂(dba)₃,

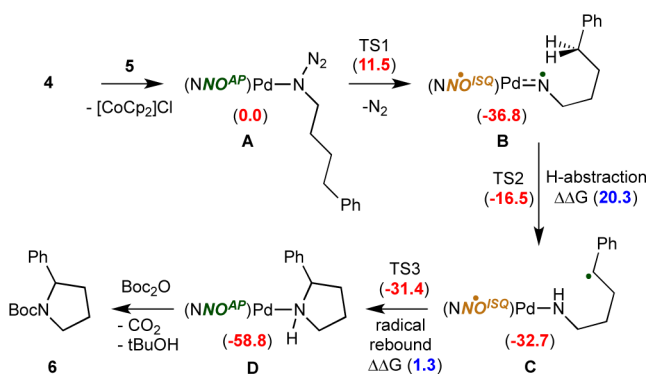
Scheme 2. Conversion of Azide **5** into Pyrrolidine **6**



Pd^{II}Cl₂(NCMe)₂, complex **2** (with and without CoCp₂), complex **3** (with and without AgPF₆ or TlPF₆), CoCp₂, or CoCp₂⁺ did not result in the formation of product **6**.¹⁷ The analogous PdCl-complex of L^{H2} was inactive, likely due to formation of iminopyridyl ligand L^{H1} via facile β -H elimination, which prohibits redox activity of the NO-fragment. Notably, in the presence of TEMPO-H, reaction of *in situ* generated **4** with azide **5** did not lead to any pyrrolidine formation, and the detection of TEMPO• by EPR spectroscopy¹⁰ supports the trapping of an active radical intermediate.

Based on these data and supported by DFT calculations, we propose the following mechanism for the intramolecular cyclization using **4** (Scheme 3). Initial chloride substitution by azide **5** gives closed-shell singlet (CSS) species **A** with an

Scheme 3. OSS Pathway from Azide **5** into **6** via Radical-Type *sp*³ C–H Amination with **4**; calculated free energies ΔG for species A–D and transition states (red) and relative barriers $\Delta\Delta G$ (blue) in kcal mol⁻¹



NNO^{AP} ligand. Loss of N₂ generates Pd-nitrene intermediate **B** that can exist in three plausible electronic states. The open-shell singlet diradical (OSS) is more stable than the CSS and triplet states by 10.6 and 5.8 kcal/mol, respectively. Furthermore, the OSS nitrene diradical **B** is most effectively generated from **A** (lowest barrier of 11.5 kcal mol⁻¹) via electron transfer from the NNO-ligand, with no redox chemistry occurring at Pd. Subsequent intramolecular H-atom abstraction forms intermediate **C** for the OSS and triplet states with barriers of 20.3 and 19.4 kcal mol⁻¹, respectively. A subsequent low barrier transition state for the radical rebound step (1.3 kcal mol⁻¹) to form **D** was found on the OSS surface. For the CSS species, direct C–H insertion of the nitrene fragment in **B** to form **D** has a higher absolute barrier than the stepwise radical process on the OSS surface (Figure 5). Reaction of intermediate **D** with

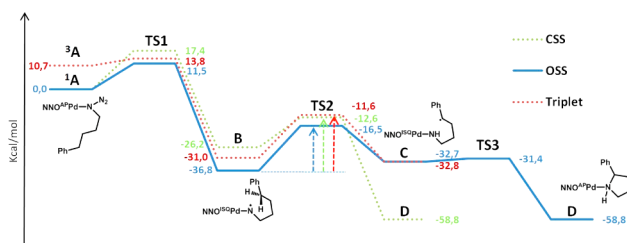


Figure 5. DFT (b3-lyp/def2-TZVP) calculated free energy profile $\Delta G_{298\text{ K}}^{\circ}$ (in kcal mol⁻¹) for C–H amination of azide complex **A** derived from **4** for the three possible spin states.

Boc₂O gives **6** and an unidentified paramagnetic Pd complex. Reaction of independently prepared **D**, by addition of pyrrolidine to **4**, with Boc₂O also generated product **6**. Using an isotopically labeled analogue of azide **5**, selectively monodeuterated at the benzylic position,¹⁰ we established a kinetic isotope effect (KIE) of 3.35 ± 0.1 for formation of **6**, which is reproduced very well by DFT calculations (KIE of 3.65). Attempts to trap a rare Pd(organo-azide) complex or a hitherto elusive (quasi)stable Pd-nitrene analogue of **B** using e.g. PhI=NNs, AdN₃, or C₆F₅N₃ did not provide a clear indication for the formation of such species.¹⁰

In conclusion, a new redox-active NNO pincer ligand L^{H2} has been synthesized and coordinated to Pd^{II}, affording paramagnetic (*S* = 1/2) complex **3** bearing the ligand-centered radical NNO^{ISQ} (L[•]), as supported by spectroscopic, X-ray crystallographic, and computational data. Reduction of **3** generates diamagnetic complex **4**, [CoCp₂][PdCl(NNO^{AP})], which is able to activate azide **5** for intramolecular C–H bond amination to produce pyrrolidine **6**. DFT calculations, isotopic labeling, and trapping experiments support a process that involves intramolecular single-electron transfer from the redox-active ligand to the substrate upon thermal activation of the organic azide, thus producing an unusual ‘nitrene-substrate radical, ligand-radical’ Pd^{II} intermediate **B** with an open-shell singlet (singlet diradical) ground state. The noninnocent NNO ligand is proposed to dictate single-electron reactivity onto Pd^{II}, enabling radical-type pathways using a metal that is normally involved in two-electron processes. This concept is likely more broadly applicable with group 8–10 metals, including for cooperative bond activation processes and catalysis.

■ ASSOCIATED CONTENT

● Supporting Information

General methods, experimental data for new compounds, NMR spectra, crystallographic details and cif files for **3** and **4**, computational data. This material is available free of charge via the Internet at <http://pubs.acs.org>.

■ AUTHOR INFORMATION

Corresponding Author

j.i.vandervlugt@uva.nl

Notes

The authors declare no competing financial interest.

■ ACKNOWLEDGMENTS

Research funded by the European Research Council (ERC Starting Grant 279097 to J.I.v.d.V.). NWO is thanked for financing the X-ray diffractometer at UU. We thank Prof. Franc Meyer (Göttingen) for access to his XRD equipment.

■ REFERENCES

- (1) (a) Stubbe, J.; van der Donk, W. A. *Chem. Rev.* **1998**, *98*, 705. (b) Harris, D. L. *Curr. Opin. Chem. Biol.* **2001**, *5*, 724. (c) Que, L.; Tolman, W. B. *Nature* **2008**, *455*, 333. (d) Kaim, W.; Schwederski, B. *Coord. Chem. Rev.* **2010**, *254*, 1580.
- (2) (a) van der Vlugt, J. I. *Eur. J. Inorg. Chem.* **2012**, 363. (b) Lyaskovskyy, V.; de Bruin, B. *ACS Catal.* **2012**, *2*, 270. (c) Dzik, W. I.; van der Vlugt, J. I.; Reek, J. N. H.; de Bruin, B. *Angew. Chem., Int. Ed.* **2011**, *50*, 3356. (d) Kaim, W. *Inorg. Chem.* **2011**, *50*, 9752. (e) Chirik, P. J.; Wieghardt, K. *Science* **2010**, *327*, 794. (f) Wong, J. L.; Sánchez, R. H.; Logan, J. C.; Zarkesh, R. A.; Ziller, J. W.; Heyduk, A. F. *Chem. Sci.* **2013**, *4*, 1906. (g) Myers, T. W.; Berben, L. A. *Chem. Commun.* **2013**, 49, 4175. (h) Smith, A. L.; Hardcastle, K. I.; Soper, J. D. *J. Am. Chem. Soc.* **2010**, *132*, 14358. (i) Sylvester, K. J.; Chirik, P. J. *J. Am. Chem. Soc.* **2009**, *131*, 8772. (j) Königsmann, M.; Donati, N.; Stein, D.; Schönberg, H.; Harmer, J.; Sreekanth, A.; Grützmacher, H. *Angew. Chem., Int. Ed.* **2007**, *46*, 3567.
- (3) Lippert, C. A.; Arnstein, S. A.; Sherill, C. D.; Soper, J. D. *J. Am. Chem. Soc.* **2010**, *132*, 3879. See also ref 2b and i.
- (4) Mono- and dinuclear Pd^{III} open-shell species: (a) Mazzotti, A. R.; Cambell, M. G.; Tang, P.; Murphy, J. M.; Ritter, T. *J. Am. Chem. Soc.* **2013**, *135*, 14012. (b) Powers, D. C.; Ritter, T. *Top. Organomet. Chem.* **2011**, *503*, 129. (c) Boisvert, L.; Denney, M. C.; Hanson, S. K.; Goldberg, K. I. *J. Am. Chem. Soc.* **2009**, *131*, 15802.
- (5) (a) Min, K. S.; Weyhermüller, T.; Bothe, E.; Wieghardt, K. *Inorg. Chem.* **2004**, *43*, 2922. (b) Ringenberg, M. R.; Kokatam, S. L.; Heiden, Z. M.; Rauchfuss, T. B. *J. Am. Chem. Soc.* **2008**, *130*, 788. (c) Deibel, N.; Schweinfurth, D.; Hohloch, S.; Delor, M.; Sazanovich, I. V.; Towrie, M.; Weinstein, J. A.; Sarkar, B. *Inorg. Chem.* **2014**, *53*, 1021.
- (6) (a) van Koten, G.; Milstein, D. *Organometallic Pincer Chemistry*; Springer: Heidelberg, 2012. (b) Gunanathan, C.; Milstein, D. *Acc. Chem. Res.* **2011**, *44*, 588. (c) van der Vlugt, J. I.; Reek, J. N. H. *Angew. Chem., Int. Ed.* **2009**, *48*, 8832. Pd(pyridyl-based pincer) species: (d) Feller, M.; Ben-Ari, E.; Iron, M. A.; Diskin-Posner, Y.; Leitius, G.; Shimon, L. J. W.; Konstantinovskii, L.; Milstein, D. *Inorg. Chem.* **2010**, *49*, 1615. (e) van der Vlugt, J. I.; Siegler, M. A.; Janssen, M.; Vogt, D.; Spek, A. L. *Organometallics* **2009**, *28*, 7025. (f) Gómez-Blanco, N.; Fernández, J. J.; Fernández, A.; Vázquez-García, D.; López-Torres, M.; Vila, J. M. *Eur. J. Inorg. Chem.* **2009**, 3071. (g) Michael, F. E.; Cochran, B. M. *J. Am. Chem. Soc.* **2006**, *128*, 4246.
- (7) Pd^{II} complexes based on 2-aminophenol: (a) Kokatam, S.-L.; Chaudhuri, P.; Weyhermüller, T.; Wieghardt, K. *Dalton Trans.* **2007**, 373. (b) Kokatam, S.; Weyhermüller, T.; Bothe, E.; Chaudhuri, P.; Wieghardt, K. *Inorg. Chem.* **2005**, *44*, 3709.
- (8) Ciganek, E. *J. Org. Chem.* **1992**, *57*, 4521.

(9) Adapted from: Bang, Z. N.; Komissarov, V. N.; Sayapin, Y. A.; Tkachev, V. V.; Shilov, G. V.; Aldoshin, S. M.; Minkin, V. I. *Russ. J. Org. Chem.* **2009**, *45*, 442.

(10) See Supporting Information for details.

(11) Sur, S. K. *J. Magn. Reson.* **1989**, *82*, 169.

(12) (a) Lippert, C.; Hardcastle, K. I.; Soper, J. D. *Inorg. Chem.* **2011**, *50*, 9864. (b) Sun, X.; Chun, H.; Hildenbrand, K.; Bothe, E.; Weyhermüller, T.; Neese, F.; Wieghardt, K. *Inorg. Chem.* **2002**, *41*, 4295. (c) Chaudhuri, P.; Verani, C. N.; Bill, E.; Bothe, E.; Weyhermüller, T.; Wieghardt, K. *J. Am. Chem. Soc.* **2001**, *123*, 2213.

(13) Review, N-centered ligand radicals in catalysis: (a) Olivos Suárez, A. I.; Lyaskovskyy, V.; Reek, J. N. H.; van der Vlugt, J. I.; de Bruin, B. *Angew. Chem., Int. Ed.* **2013**, *52*, 12510. See also: (b) Lyaskovskyy, V.; Olivos Suárez, A. I.; Lu, H.; Jiang, H.; Zhang, X. P.; de Bruin, B. *J. Am. Chem. Soc.* **2011**, *133*, 12264. Proposed Pd-nitrene or -imido species: (c) Mooibroek, T. J.; Schoon, L.; Bouwman, E.; Drent, E. *Chem.—Eur. J.* **2011**, *17*, 13318. (d) Berry, J. F. *Comm. Inorg. Chem.* **2009**, *30*, 28.

(14) Pd(organo-azide) complexes are very rare: (a) Barz, M.; Herdtweck, E.; Thiel, W. *Angew. Chem., Int. Ed.* **1998**, *37*, 2262. (b) Besenyi, G.; Párkányi, L.; Foch, I.; Simándi, L. I. *Angew. Chem., Int. Ed.* **2000**, *39*, 956.

(15) Reviews: (a) Jeffrey, J. L.; Sarpong, R. *Chem. Sci.* **2013**, *4*, 4092. (b) Roizen, J. L.; Harvey, M. E.; Du Bois, J. *Acc. Chem. Res.* **2012**, *45*, 911. (c) Gephart, R. T.; Warren, T. H. *Organometallics* **2012**, *31*, 7727.

(16) Hennessy, E. T.; Betley, T. A. *Science* **2013**, *340*, 591.

(17) Pd₂dba₃ did lead to full conversion, but only to 7. Pd-black is observed after reaction; we propose that a decomposition product of **4** is responsible for the formation of **7**.